Guidance and Control for UAV Aerial Refueling Docking Based on Dynamic Inversion with L_1 Adaptive Augmentation

Yuan Suozhong(袁锁中)*, *Zhen Ziyang*(甄子洋), *Jiang Ju*(江驹)

College of Automation Engineering, Nanjing University of Aeronautics and Astronautics, Nanjing 210016, P. R. China

(Received 4 November 2014; revised 24 December 2014; accepted 12 January 2015)

Abstract: The guidance and control for UAV aerial refueling docking based on dynamic inversion with L_1 adaptive augmentation is studied. In order to improve the tracking performance of UAV aerial refueling docking, a guidance algorithm is developed to satisfy the tracking requirement of position and velocity, and it generates the UAV flight control loop commands. In flight control loop, based on the 6-DOF nonlinear model, the angular rate loop and the attitude loop are separated based on time-scale principle and the control law is designed using dynamic inversion. The throttle control is also derived from dynamic inversion method. Moreover, an L_1 adaptive augmentation is developed to compensate for the undesirable effects of modeling uncertainty and disturbance. Nonlinear digital simulations are carried out. The results show that the guidance and control system has good tracking performance and robustness in achieving accurate aerial refueling docking.

Key words: aerial refueling; dynamic inversion; guidance algorithm; L_1 adaptive augmentation

CLC number: V249 **Document code**: A **Article ID**: 1005-1120(2015)01-0035-07

0 Introduction

Unmanned aerial vehicles (UAVs) have been widely deployed in international military conflict recently to perform different missions ranging from reconnaissance, intelligence acquisition, to actual combat missions. Aerial refueling can extend the range, shorten the response time, and extend loiter time of UAVs. The UAV aerial refueling has become the trend of the future development of UAV technology. One of the required technologies is the ability to autonomously docking with the tanker[1-2]. Probe-and-drogue refueling method is a good choice for UAV aerial refueling. It requires a good autonomous three-dimensional tracking controller. But this is extremely difficult due to the aerodynamic coupling among the two aircraft and the drogue.

The problem of aerial refueling flight control has been intensively addressed over the past decades. PID control laws for aerial refueling are used in Ref. [3] without considering the effect of the trailing vortex in the simulation. Station keeping control system for aerial refueling using quantitative feedback theory was designed to take care of the wind gust and fuel-transferring disturbances in Ref. [4]. In Ref. [5] the authors studied the applicability of proportional navigation guidance and line-of-sight angle control in aerial refueling. An optimal controller with a control-rate-weighting controller was applied to track and dock with a stationary drogue under the influence of Dryden light turbulence[6]. All those were studied based on the linear model of the receiver aircraft.

To copy with the trailing vortex and disturbance, model reference adaptive control (MRAC) architecture with neural networks were designed in Ref. [7], but it only studied the longitudinal channel. In order to improve the transient performance of aerial refueling tracking control, a

* **Corresponding author**: Yuan Suozhong, Associate Researcher, E-mail: szyuan@nuaa.edu.cn.

How to cite this article: Yuan Suozhong, Zhen Ziyang, Jiang Ju. Guidance and control for UAV aerial refueling docking based on dynamic inversion with L_1 adaptive augmentation[J]. Trans. Nanjing U. Aero. Astro., 2015,32(1):35-41. http://dx.doi.org/10.16356/j.1005-1120.2015.01.035

novel L_1 neural network adaptive control were studied in Refs. [8—9]. Based on linear model, the L_1 controller was designed for each of the three position-separation axes. Simulation showed it had good robust tracking performance with good transient response. But practically, The UAV dynamics is a full nonlinear six-DOF model[10]. In this paper, we propose a nonlinear adaptive control law for UAV aerial refueling guidance and control using nonlinear dynamic inversion with L_1 adaptive augmentation.

1 Controller Structure for UAV Aerial Refueling Docking

The summary of the entire guidance and control loop for UAV autonomous aerial refueling docking is shown in Fig. 1, including a guidaning law module, a UAV flight control module, a dynamic module of the UAV and a module of relative motion between UAV and a tanker aircraft.

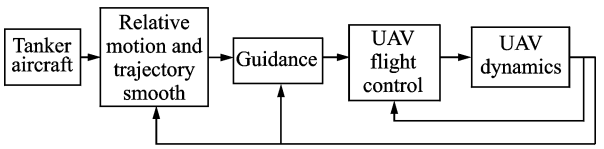

Fig. 1 Block diagram of guidance and control structure for UAV aerial refueling docking

2 Guidance Law

The ultimate goal of UAV aerial refueling docking is to control the UAV to track the tanker aircraft, approach and get connected with the drogue, while matching the tanker′s heading, and airspeed.

So the control objective can be given as

$$\begin{bmatrix} x \\ y \\ z \end{bmatrix} \rightarrow \begin{bmatrix} x_d \\ y_d \\ z_d \end{bmatrix}, \begin{bmatrix} V \\ \gamma \\ \chi \end{bmatrix} \rightarrow \begin{bmatrix} V_d \\ \gamma_d \\ \chi_d \end{bmatrix} \tag{1}$$

where x, y, z describe the UAV′s position in inertial coordinate axes, and x_d, y_d, z_d the desired coordinates of the UAV in fixed inertial frame. In aerial refueling it can be treated as the drogue′s position in inertial coordinate axes. V, γ, χ are the UAV airspeed, longitudinal flight path angle and lateral path angle, respectively, and V_d, γ_d, χ_d the tanker airspeed, longitudinal flight path angle and lateral path angle, respectively.

Defining two vectors $\boldsymbol{Z}_1$ and $\boldsymbol{Z}_2$

$$\boldsymbol{Z}_1 = [x \quad y \quad z]^{\mathrm{T}}, \ \boldsymbol{Z}_2 = [V \quad \gamma \quad \chi]^{\mathrm{T}} \tag{2}$$

Considering a tracking error formulation as given below

$$\Delta \boldsymbol{Z} = \Delta \dot{\boldsymbol{Z}}_1 + \boldsymbol{K}_1 \Delta \boldsymbol{Z}_1 \tag{3}$$

where

$$\Delta \boldsymbol{Z}_1 = \begin{bmatrix} x - x_d \\ y - y_d \\ z - z_d \end{bmatrix}, \ \Delta \dot{\boldsymbol{Z}}_1 = \begin{bmatrix} \dot{x} - \dot{x}_d \\ \dot{y} - \dot{y}_d \\ \dot{z} - \dot{z}_d \end{bmatrix}$$

$$\boldsymbol{K}_1 = \begin{bmatrix} k_{11} & 0 & 0 \\ 0 & k_{12} & 0 \\ 0 & 0 & k_{13} \end{bmatrix} \tag{4}$$

where $\Delta \boldsymbol{Z}$ is the tracking error, and $\boldsymbol{K}_1$ the gain matrix of the tracking system. The objective is to make the tacking error zero so that the guidance requirement can be fulfilled.

From the tracking error formulation it is assured that as $\Delta \boldsymbol{Z} \rightarrow 0$, it satisfies $\Delta \dot{\boldsymbol{Z}}_1 \rightarrow 0, \Delta \boldsymbol{Z}_1 \rightarrow 0$.

The trajectory equation of UAV in velocity axes is

$$\begin{bmatrix} \dot{x} \\ \dot{y} \\ \dot{z} \end{bmatrix} = \begin{bmatrix} V\cos\gamma\cos\chi \\ V\cos\gamma\sin\chi \\ -V\sin\gamma \end{bmatrix} \tag{5}$$

And Eq. (5) can be rewritten as

$$\dot{\boldsymbol{Z}}_1 = f(\boldsymbol{Z}_2) \tag{6}$$

Thus, the error $\Delta \dot{\boldsymbol{Z}}_1$ can be expressed as

$$\Delta \dot{\boldsymbol{Z}}_1 = \frac{\partial f(\boldsymbol{Z}_2)}{\partial \boldsymbol{Z}_2} \Delta \boldsymbol{Z}_2 = \boldsymbol{A} \Delta \boldsymbol{Z}_2 \tag{7}$$

where

$$\boldsymbol{A} = \begin{bmatrix} \cos\gamma\cos\chi & -V\sin\gamma\cos\chi & -V\cos\gamma\sin\chi \\ \cos\gamma\sin\chi & -V\sin\gamma\sin\chi & V\cos\gamma\cos\chi \\ -\sin\gamma & -V\cos\gamma & 0 \end{bmatrix} \tag{8}$$

In the process of aerial refueling, it generally satisfies $\gamma < 90^{\circ}$. Therefore, matrix $\boldsymbol{A}$ will be nonsingular. We can assure that as $\Delta \dot{\boldsymbol{Z}}_1 \rightarrow 0$, $\Delta \boldsymbol{Z}_2 \rightarrow 0$. $\Delta \boldsymbol{Z}_1 \rightarrow 0$ implies that the required position is achieved and $\Delta \boldsymbol{Z}_2 \rightarrow 0$ implies that the velocity is also achieved.

The aim of the guidance loop is to make $\Delta \boldsymbol{Z} \rightarrow 0$ and thereby generate the required com-

mands for UAV flight control system.

The error dynamics equation is

$$\Delta\dot{\boldsymbol{Z}}+\boldsymbol{K}_2\Delta\boldsymbol{Z}=0 \tag{9}$$

where

$$\boldsymbol{K}_2=\begin{bmatrix}k_{21}&0&0\\0&k_{22}&0\\0&0&k_{23}\end{bmatrix}$$

From Eq. (3) one gets

$$\Delta\dot{\boldsymbol{Z}}=\Delta\ddot{\boldsymbol{Z}}_1+\boldsymbol{K}_1\Delta\dot{\boldsymbol{Z}}_1=\begin{bmatrix}\ddot{x}-\ddot{x}_{\mathrm{d}}\\\ddot{y}-\ddot{y}_{\mathrm{d}}\\\ddot{z}-\ddot{z}_{\mathrm{d}}\end{bmatrix}+\boldsymbol{K}_1\begin{bmatrix}\dot{x}-\dot{x}_{\mathrm{d}}\\\dot{y}-\dot{y}_{\mathrm{d}}\\\dot{z}-\dot{z}_{\mathrm{d}}\end{bmatrix} \tag{10}$$

Differentiating Eq. (5) gains

$$\begin{bmatrix}\ddot{x}\\\ddot{y}\\\ddot{z}\end{bmatrix}=\frac{\mathrm{d}}{\mathrm{d}t}\begin{bmatrix}V\cos\gamma\cos\chi\\V\cos\gamma\sin\chi\\-V\sin\gamma\end{bmatrix}=\boldsymbol{A}\begin{bmatrix}\dot{V}\\\dot{\gamma}\\\dot{\chi}\end{bmatrix} \tag{11}$$

From Eqs. (9—11), one obtains

$$\boldsymbol{A}\begin{bmatrix}\dot{V}\\\dot{\gamma}\\\dot{\chi}\end{bmatrix}-\begin{bmatrix}\ddot{x}_{\mathrm{d}}\\\ddot{y}_{\mathrm{d}}\\\ddot{z}_{\mathrm{d}}\end{bmatrix}+\boldsymbol{K}_1\begin{bmatrix}\dot{x}-\dot{x}_{\mathrm{d}}\\\dot{y}-\dot{y}_{\mathrm{d}}\\\dot{z}-\dot{z}_{\mathrm{d}}\end{bmatrix}+\boldsymbol{K}_2\left(\begin{bmatrix}\dot{x}-\dot{x}_{\mathrm{d}}\\\dot{y}-\dot{y}_{\mathrm{d}}\\\dot{z}-\dot{z}_{\mathrm{d}}\end{bmatrix}+\boldsymbol{K}_1\begin{bmatrix}x-x_{\mathrm{d}}\\y-y_{\mathrm{d}}\\z-z_{\mathrm{d}}\end{bmatrix}\right)=0 \tag{12}$$

Generally, in the process of docking, the tanker flies in a straight level flight with a constant speed, i. e., $[\ddot{x}_{\mathrm{d}}\quad\ddot{y}_{\mathrm{d}}\quad\ddot{z}_{\mathrm{d}}]^{\mathrm{T}}\approx 0$. Therefore, Eq. (13) is obtained.

$$\begin{bmatrix}\dot{V}_{\mathrm{c}}\\\dot{\gamma}_{\mathrm{c}}\\\dot{\chi}_{\mathrm{c}}\end{bmatrix}=\boldsymbol{A}^{-1}\left(\left(\boldsymbol{K}_1+\boldsymbol{K}_2\begin{bmatrix}V\cos\gamma\cos\chi\\V\cos\gamma\sin\chi\\-V\sin\gamma\end{bmatrix}-\begin{bmatrix}\dot{x}_{\mathrm{d}}\\\dot{y}_{\mathrm{d}}\\\dot{z}_{\mathrm{d}}\end{bmatrix}\right)+\boldsymbol{K}_1\boldsymbol{K}_2\begin{bmatrix}x-x_{\mathrm{d}}\\y-y_{\mathrm{d}}\\z-z_{\mathrm{d}}\end{bmatrix}\right) \tag{13}$$

The vertical and the lateral acceleration components can be related to the flight path angle using a point mass model of the equations of motion

$$-a_z=V_{\mathrm{UAV}}\dot{\gamma}=\frac{1}{m}(L+T\sin\alpha)\cos\phi-g\cos\gamma \tag{14}$$

$$a_y=V\dot{\chi}\cos\gamma=\frac{1}{m}(L+T\sin\alpha)\sin\phi \tag{15}$$

where m and g are the UAV mass and gravity constant, respectively; L, T the lift and thrust forces, and α, ϕ the angle of attack and the bank angle, respectively.

Solving Eqs. (14—15), one has

$$\phi_{\mathrm{c}}=\arctan\left(\frac{a_y}{a_z+g\cos\gamma}\right) \tag{16}$$

$$\alpha_{\mathrm{c}}=\frac{m\sqrt{(-a_z+g\cos\gamma)^2+(a_y)^2}-T\sin\alpha}{QSC_{L_\alpha}}+\alpha_0 \tag{17}$$

where Q is the dynamics pressure, S the wing area, C_{L_α} the lift coefficient, and α_0 the trim angle of attack.

3 UAV Flight Control Law Based on Dynamic Inversion

A two-time-scale approach[11] is implemented in Fig. 2. A "fast mode" control in which the inverse system outputs is the UAV commands, such as aileron, elevator and rudder deflections, while its inputs are fast-mode's commands concerned with roll rate p, pitch rate q, and yaw rate r. Moreover, there is a "slow mode" control, in which the inverse system outputs corresponds to the fast-mode's commands p,q,r, while the inputs are slow-mode's commands concerned with angle of attack, bank angle, and sideslip angle. The α, ϕ commands are obtained from the guidance loop.

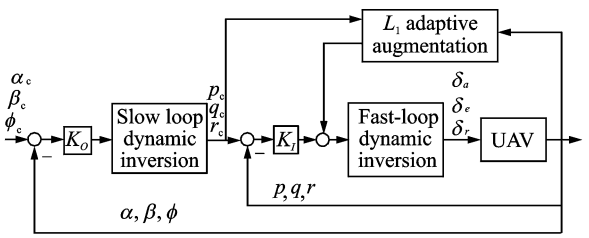

Fig. 2 Block diagram of angle control system of UAV

The desired dynamic equation for the slow loop is

$$\begin{bmatrix}\dot{\alpha}_{\mathrm{c}}\\\dot{\beta}_{\mathrm{c}}\\\dot{\phi}_{\mathrm{c}}\end{bmatrix}=\boldsymbol{K}_O\begin{bmatrix}(\alpha_{\mathrm{c}}-\alpha)\\(\beta_{\mathrm{c}}-\beta)\\(\phi_{\mathrm{c}}-\phi)\end{bmatrix} \tag{18}$$

where $\dot{\alpha}_{\mathrm{c}}$, $\dot{\beta}_{\mathrm{c}}$, $\dot{\phi}_{\mathrm{c}}$ are the desired values. $\boldsymbol{K}_O$ is a diagonal matrix representing the bandwidth of each loop.

The angular dynamics is given by

$$[\dot{\alpha} \quad \dot{\beta} \quad \dot{\phi}]^{\mathrm{T}} = \boldsymbol{f}_1(x) + \boldsymbol{g}_1(x)[p \quad q \quad r]^{\mathrm{T}} \tag{19}$$

where

$$\boldsymbol{f}_1 = \begin{bmatrix} \frac{1}{mV\cos\beta}(-T\sin\alpha - L + mg_z) \\ \frac{1}{mV}(-T\cos\alpha\sin\beta + Y + mg_y) \\ 0 \end{bmatrix}$$

$$\boldsymbol{g}_1 = \begin{bmatrix} -\cos\alpha\tan\beta & 1 & -\sin\alpha\tan\beta \\ \sin\alpha & 0 & -\cos\alpha \\ 1 & \tan\theta\sin\phi & \tan\theta\cos\phi \end{bmatrix}$$

$$g_z = g(\sin\alpha\sin\theta + \cos\alpha\cos\phi\cos\theta)$$

$$g_y = g(\sin\theta\cos\alpha\sin\beta + \sin\phi\cos\theta\cos\beta - \cos\phi\cos\theta\sin\alpha\sin\beta)$$

Solving Eq. (19) for $(p,q,r)^{\mathrm{T}}$ and replacing $(p,q,r)^{\mathrm{T}}$ with $(p_{\mathrm{c}},q_{\mathrm{c}},r_{\mathrm{c}})^{\mathrm{T}}$ and $(\dot{\alpha},\dot{\beta},\dot{\phi})^{\mathrm{T}}$ with $(\dot{\alpha}_{\mathrm{c}},\dot{\beta}_{\mathrm{c}},\dot{\phi}_{\mathrm{c}})^{\mathrm{T}}$, we gets

$$\begin{bmatrix} p_{\mathrm{c}} \\ q_{\mathrm{c}} \\ r_{\mathrm{c}} \end{bmatrix} = \boldsymbol{g}_1^{-1}\left(\boldsymbol{K}_O \begin{bmatrix} \alpha_{\mathrm{c}} - \alpha \\ \beta_{\mathrm{c}} - \beta \\ \phi_{\mathrm{c}} - \phi \end{bmatrix} - \boldsymbol{f}_1\right) \tag{20}$$

The fast loop dynamics of UAV is given by

$$\begin{bmatrix} \dot{p} \\ \dot{q} \\ \dot{r} \end{bmatrix} = \boldsymbol{f}_2(\boldsymbol{x}) + \boldsymbol{g}_2(x) \begin{bmatrix} L \\ M \\ N \end{bmatrix} \tag{21}$$

where

$$\boldsymbol{f}_2 = \begin{bmatrix} c_1 rq + c_2 pq \\ c_5 pr - c_6 p^2 + c_6 r^2 \\ c_8 pq - c_2 rq \end{bmatrix}$$

$$\boldsymbol{g}_2 = \begin{bmatrix} c_3 & 0 & c_4 \\ 0 & c_7 & 0 \\ c_4 & 0 & c_9 \end{bmatrix}$$

$$c_1 = \frac{(I_y - I_z)I_z - I_{xz}^2}{I_z - I_{xz}^2},\ c_2 = \frac{(I_x - I_y + I_z)I_{xz}}{I_z - I_{xz}^2}$$

$$c_3 = \frac{I_z}{I_z - I_{xz}^2},\ c_4 = \frac{I_{xz}}{I_z - I_{xz}^2},\ c_5 = \frac{I_z - I_x}{I_z - I_{xz}^2},\ c_6 = \frac{I_{xz}}{I_y},$$

$$c_7 = \frac{1}{I_y},\ c_8 = \frac{(I_x - I_y)I_x + I_{xz}^2}{I_z - I_{xz}^2},\ c_9 = \frac{I_x}{I_z - I_{xz}^2}$$

The equation between the control surface and the moment is

$$\begin{bmatrix} L \\ M \\ N \end{bmatrix} = \boldsymbol{f}_3 + \boldsymbol{g}_3 \begin{bmatrix} \delta_e \\ \delta_a \\ \delta_r \end{bmatrix} \tag{22}$$

where

$$\boldsymbol{f}_3 = \begin{bmatrix} \frac{1}{2}\rho V^2 Sb(C_{l_0} + C_{l_\beta}\beta + C_{l_p}\frac{b}{2V}p + C_{l_r}\frac{b}{2V}r) \\ \frac{1}{2}\rho V^2 Sc(C_{m_0} + C_{m_\alpha}\alpha + C_{m_q}\frac{c}{2V}q) \\ \frac{1}{2}\rho V^2 Sb(C_{n_0} + C_{n_\beta}\beta + C_{n_p}\frac{b}{2V}p + C_{n_r}\frac{b}{2V}r) \end{bmatrix}$$

$$\boldsymbol{g}_3 = \begin{bmatrix} 0 & C_{l_{\delta_a}} & C_{l_{\delta_r}} \\ C_{m_{\delta_e}} & 0 & 0 \\ 0 & C_{n_{\delta_a}} & C_{n_{\delta_r}} \end{bmatrix}$$

From Eqs. (21—22), one obtains

$$\begin{bmatrix} \dot{p} \\ \dot{q} \\ \dot{r} \end{bmatrix} = (\boldsymbol{f}_2 + \boldsymbol{g}_2\boldsymbol{f}_3) + \boldsymbol{g}_2\boldsymbol{g}_3 \begin{bmatrix} \delta_e \\ \delta_a \\ \delta_r \end{bmatrix} \tag{23}$$

Defining the desired dynamic equations for the fast loop as

$$\begin{bmatrix} \dot{p}_{\mathrm{c}} \\ \dot{q}_{\mathrm{c}} \\ \dot{r}_{\mathrm{c}} \end{bmatrix} = \boldsymbol{K}_I \begin{bmatrix} p_{\mathrm{c}} - p \\ q_{\mathrm{c}} - q \\ r_{\mathrm{c}} - r \end{bmatrix} \tag{24}$$

where $\boldsymbol{K}_I$ is a diagonal matrix which represents the bandwidth of each angular rate loop.

Solving Eq. (23) for $[\delta_e \quad \delta_a \quad \delta_r]^{\mathrm{T}}$, and replacing $(\dot{p},\dot{q},\dot{r})^{\mathrm{T}}$ with $(\dot{p}_{\mathrm{c}},\dot{q}_{\mathrm{c}},\dot{r}_{\mathrm{c}})^{\mathrm{T}}$, one obtains the control surface command signal

$$\begin{bmatrix} \delta_{e_{\mathrm{c}}} \\ \delta_{a_{\mathrm{c}}} \\ \delta_{r_{\mathrm{c}}} \end{bmatrix} = (\boldsymbol{g}_2\boldsymbol{g}_3)^{-1}\left(\boldsymbol{K}_2 \begin{bmatrix} \dot{p}_{\mathrm{c}} \\ \dot{q}_{\mathrm{c}} \\ \dot{r}_{\mathrm{c}} \end{bmatrix} - \boldsymbol{f}_2 - \boldsymbol{g}_2\boldsymbol{f}_3\right) \tag{25}$$

4 L_1 Adaptive Augmentation

If the model uncertainties and disturbance are considered, the performance of the control law designed in the above section will be degraded. Here one designs a L_1 adaptive controller to compensate the effects of the disturbance and model uncertainties[12].

For simplification, Eq. (23) can be written as

$$\dot{\boldsymbol{\omega}} = \boldsymbol{f}_4(\boldsymbol{x}) + \boldsymbol{g}_4(\boldsymbol{x})\boldsymbol{u}_\delta \tag{26}$$

where $\boldsymbol{\omega} = [p \quad q \quad r]^{\mathrm{T}}$, $\boldsymbol{u}_\delta = [\delta_e \quad \delta_a \quad \delta_r]^{\mathrm{T}}$. If considering the disturbance and model uncertainties, Eq. (26) becomes

$$\dot{\boldsymbol{\omega}} = \boldsymbol{f}_{4_0}(x) + \Delta\boldsymbol{f}_4(x) + (\boldsymbol{g}_{4_0}(x) + \Delta\,\boldsymbol{g}_4(x))\boldsymbol{u}_\delta + \boldsymbol{d}(x) \tag{27}$$

where $\boldsymbol{d}(x)$ is the disturbance, $\boldsymbol{f}_{4_0}(x)$, $\boldsymbol{g}_{4_0}(x)$ are the known component of the model dynamics, and $\Delta\boldsymbol{f}_4$, $\Delta\boldsymbol{g}_4$ the unknown components of the UAV dynamics. Rearrange the above, one has

$$\dot{\boldsymbol{\omega}} = \boldsymbol{f}_{4_0}(x) + \boldsymbol{g}_{4_0}(x)\boldsymbol{u}_\delta + \boldsymbol{\sigma}(x) \tag{28}$$

$$\boldsymbol{\sigma}(x) = \Delta\boldsymbol{f}_4(x) + \Delta\boldsymbol{g}_4(x)\boldsymbol{u}_\delta + \boldsymbol{d}(x) \tag{29}$$

Solving Eq. (28), the surface command can be attained

$$\boldsymbol{u}_\delta = \boldsymbol{g}_{4_0}^{-1}(x)(\boldsymbol{v} - \boldsymbol{f}_{4_0}(x) - \boldsymbol{\sigma}(x)) \tag{30}$$

Let the pseudoinput be

$$\boldsymbol{v} = \boldsymbol{u}_{\text{lin}} + \boldsymbol{u}_{\text{ad}} = \boldsymbol{K}_I(\boldsymbol{\omega}_{\text{c}} - \boldsymbol{\omega}) + \boldsymbol{u}_{\text{ad}} \tag{31}$$

where $\boldsymbol{u}_{\text{lin}} = \boldsymbol{K}_I(\boldsymbol{\omega}_{\text{c}} - \boldsymbol{\omega})$ is the baseline control. It guarantees the tracking performance with no need to consider the disturbance and model uncertainties. $\boldsymbol{u}_{\text{ad}}$ is the adaptive output which compensates the disturbance and model uncertainties

Substituting Eqs. (30—31) into Eq. (28), one gets

$$\dot{\boldsymbol{\omega}} = -\boldsymbol{K}_I\boldsymbol{\omega} + \boldsymbol{I}_3(\boldsymbol{K}_I\boldsymbol{\omega}_{\text{c}} + \boldsymbol{u}_{\text{ad}} + \boldsymbol{\sigma}) \tag{32}$$

It can be written as

$$\dot{\boldsymbol{\omega}} = \boldsymbol{A}_{\text{m}}\omega + \boldsymbol{B}_{\text{m}}(\boldsymbol{K}_I\boldsymbol{\omega}_{\text{c}} + \boldsymbol{u}_{\text{ad}} + \boldsymbol{\sigma}) \tag{33}$$

where

$$\boldsymbol{A}_{\text{m}} = -\boldsymbol{K}_I, \boldsymbol{B}_m = \boldsymbol{I}_3$$

The L_1 adaptive element should estimate the uncertainties. The following is the state predicator's dynamics[8]

$$\dot{\hat{\boldsymbol{\omega}}} = \boldsymbol{A}_{\text{m}}\hat{\boldsymbol{\omega}} + \boldsymbol{B}_{\text{m}}(\boldsymbol{K}_I\boldsymbol{\omega}_{\text{c}} + \boldsymbol{u}_{\text{ad}} + \hat{\boldsymbol{\sigma}}) + \boldsymbol{K}_{\text{S}}\tilde{\boldsymbol{\omega}} \tag{34}$$

where $\tilde{\boldsymbol{\omega}} = \hat{\boldsymbol{\omega}} - \boldsymbol{\omega}$ is the error between the system states and the predicted states. The term $\boldsymbol{K}_{\text{S}}\tilde{\boldsymbol{\omega}}$ is used to speed up the predication error dynamics.

The predication error dynamics can be written as

$$\dot{\tilde{\boldsymbol{\omega}}} = \boldsymbol{A}_{\text{m}}\tilde{\boldsymbol{\omega}} + \boldsymbol{B}_{\text{m}}\tilde{\boldsymbol{\sigma}} + \boldsymbol{K}_{\text{S}}\tilde{\boldsymbol{\omega}} \tag{35}$$

where matrix $\boldsymbol{K}_{\text{S}}$ is chosen to guarantee the equation $\boldsymbol{A}_{\text{s}} = \boldsymbol{A}_{\text{m}} + \boldsymbol{K}_{\text{s}}$ stable.

The adaptation law is defined by[8]

$$\hat{\boldsymbol{\sigma}}(t) = -\boldsymbol{B}_{\text{m}}^{-1}(\boldsymbol{A}_{\text{s}}^{-1} - \boldsymbol{I}_3))^{-1}(e^{\boldsymbol{A}_{\text{s}}T_{\text{s}}}\tilde{x}(iT_s)$$

$$t \in [iT_{\text{s}}, (i+1)T_{\text{s}}],\ i = 0, 1, 2, \cdots \tag{36}$$

where T_{s} is the adaption update rate, which is limited in real application by given hardware.

The control signal to be provided by the adaptive augmentation is

$$\boldsymbol{u}_{\text{ad}}(s) = -\boldsymbol{C}(s)\hat{\boldsymbol{\sigma}}(s) \tag{37}$$

where $\boldsymbol{C}(s)$ can be chosen as a strictly proper filter with second-order dynamics $\boldsymbol{C}(s) = \left(\frac{\omega_{\text{c}0}^2}{s^2 + 2\xi_{\text{c}0}\omega_{\text{c}0}s + \omega_{\text{c}0}^2}\right)\boldsymbol{I}_3$.

5 Velocity Control Law

In order to make UAV track the drogue, the forward velocity should be controlled.

The dynamics of velocity is

$$\dot{V} = \frac{T\sin\alpha\cos\beta - D}{m} - g\sin\gamma \tag{38}$$

where D is the Drag force. From Eq. (38), the thrust command is obtained

$$T = \frac{m\dot{V}_{\text{c}} + mg\sin\gamma + D}{\sin\alpha\cos\beta} \tag{39}$$

Thereby

$$\delta_T = T/T_{\max} \tag{40}$$

6 Simulations

A 6-DOF model of the UAV is used in the simulations. The tanker aircraft is in a steady level straight flight. It is assumed that the aircraft flies toward north. The UAV's trim values are $V_0 = 200$ m/s, $z_0 = -5\,000$ m, $\delta_{T_0} = 37\%$, $\delta_{e_0} = -2.77°$. The drogue's radius is $r_{\text{d}} = 0.3$ m. The drogue lies in (−5 m, 5 m, 3 m) relative to the center of gravity of the tanker. The UAV flies behind and below the tanker, its initial relative position to the tanker in initial coordinate is (−100 m, 50 m, 50 m). To keep the UAV smoothly track the tanker, a reference trajectory generator is used to smooth the distance command, which was discussed in Ref. [6]. The tracking precision performance index is defined as $R = \| [y_{\text{d}}(t_f) \quad z_{\text{d}}(t_f)]^{\text{T}} - [y(t_f) \quad z(t_f)]^{\text{T}} \|$. Fig. 3 shows the closed-loop trajectories in each axis based on the dynamic inversion controller. The solid lines are the responses of system only under dynamics inversion control without considering any uncertainties and disturbance. In this case, $R = 0.21$. It satisfies the requirement of docking. When considering the disturbance moment induced by the tanker wake vortex and at-

mosphere turbulence[9], the responses are shown in Fig. 3 (the dashed line). And $R=1.2$, it does not satisfy the docking requirement. Fig. 4 and Fig. 5 are the corresponding time history of the UAV state and control variables (the dashed lines).

The dotted lines in Fig. 3 show the closed-loop trajectories in each axis based on the dynamic

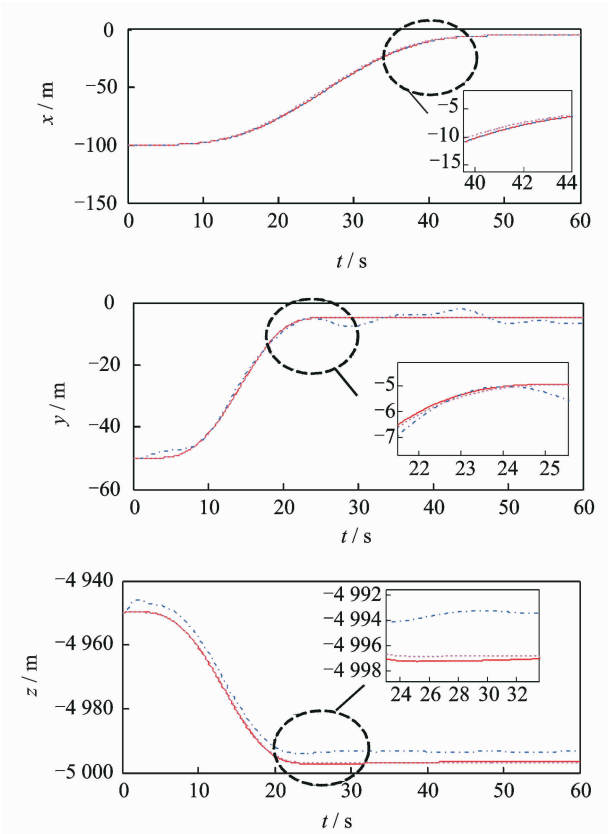

Fig. 3 Trajectory tracking for UAV aerial refueling

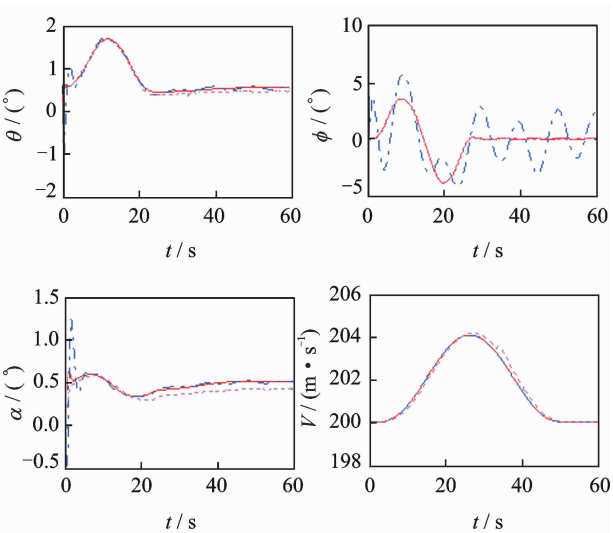

Fig. 4 State variables for UAV aerial refueling

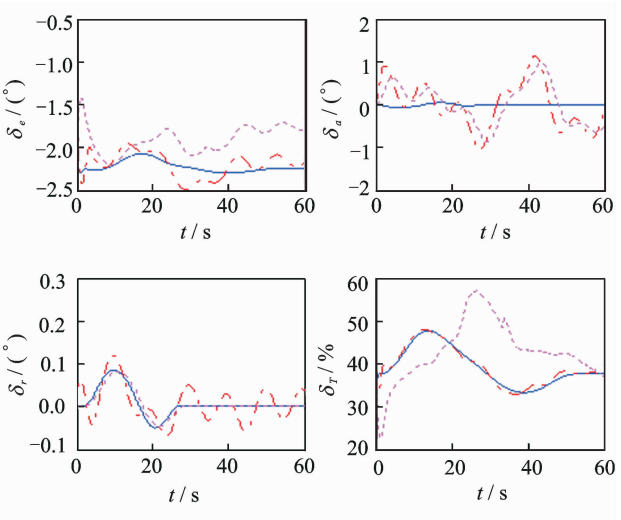

Fig. 5 Control signals for UAV aerial refueling

inversion control with L_1 adaptation augmentation in the model uncertainties and disturbance condition. In this case, $R=0.197\ 5$ satisfies the requirement of docking. Figs. 4, 5 (dotted lines) are the corresponding time history of the UAV state and control variables.

7 Conclusions

The guidance and control system for UAV aerial refueling docking is developed. The dynamic inversion method is extremely effective without any linear approximation. The L_1 augmented adaptive control compensates the model uncertainties, like inversion error, disturbance and parameters changes. Simulation shows that tracking performance and robustness for UAV aerial refueling docking with the designed system are guaranteed in the presence of model uncertainties and disturbance.

Acknowledgements

This work was supported by the National Natural Science Foundation of China (No. 61273050) and the Aeronautical Science Foundation of China (No. 20121352026).

References:

[1] Joseph P N, Jacob L H. Automated aerial refueling: Extending the effectiveness of unmanned air vehicles [R]. AIAA -2005-6005, 2005.

[2] Dibley R P, Allen M J, Nabaa N, et al. Autonomous

airborne refueling demonstration, phase I flight-test results[R]. NASA/TM-2007-214632, 2007.

[3] Ross S M, Pachter M, Jacques D R, et al. Autonomous aerial refueling based on the tanker reference frame[C]// 2006 IEEE Aerospace Conference. [S. l.]:Big Sky, M T:IEEE,2006.

[4] Pachter M, Houpis C, Trosen D. Design of an air-to-air automatic refueling flight control system using quantitative feedback theory[J]. International Journal of Robust and Nonlinear Control, 1997, 7(6): 561-580.

[5] Yoshimasa O, Takeshi K. Flight control for automatic aerial refueling via PNG and LOS angle control [R]. AIAA-2005-6268, 2005.

[6] Tandale M D, Bowers R, Valasek J. Trajectory tracking controller for vision-based probe and drogue autonomous aerial refueling[J]. AIAA Journal of Guidance, Control, and Dynamics, 2006, 29(4): 846-857.

[7] Stepanyan V, Lavretsky E, Hovakimyan N. Aerial refueling autopilot design methodology: Application to F-16 aircraft model[C]// AIAA Guidance, Navigation, and Control Conference, Providence. RI, AIAA Paper 2004-5321,2004.

[8] Wang J. Verifiable adaptive control solutions for flight control applications[D]. Virginia: Virginia Polytechnic Institute and State University, 2009.

[9] Wang J, Vijay P, Cao C. Novel L_1 adaptive control methodology for aerial refueling with guaranteed transient performance [J]. Journal of Guidance, Control, and Dynamics, 2008, 31(1): 182-192.

[10] Dogan A. Nonlinear control for reconfiguration of unmanned aerial vehicle formation[J]. Journal of Guidance, Control, and Dynamics, 2005, 28(4): 667-677.

[11] Pedro J O, Panday A, Dala L. A nonlinear dynamic inversion-based neurocontroller for unmanned combat aerial vehicles during aerial refueling[J]. International Journal of Applied Mathematics and Computer Science, 2013, 23(1):75-90.

[12] Bichlmeier M, Holzapfel F. L_1 adaptive augmentation of a helicopter baseline controller[C]// AIAA Guidance, Navigation, and Control (GNC) Conference. Boston, MA: AIAA 2013-4855,2013.

(Executive editor: Zhang Tong)